

Mutual Information-oriented ISAC Beamforming Design for Large Dimensional Antenna Array

Shanfeng Xu, Yanshuo Cheng, Siqiang Wang, Xinyi Wang, *Member, IEEE*,
Zhong Zheng, *Member, IEEE*, Zesong Fei, *Senior Member, IEEE*

Abstract

In this paper, we study the beamforming design for multiple-input multiple-output (MIMO) ISAC systems, with the weighted mutual information (MI) comprising sensing and communication perspectives adopted as the performance metric. In particular, the weighted sum of the communication mutual information and the sensing mutual information is shown to asymptotically converge to a deterministic limit when the number of transmit and receive antennas grow to infinity. This deterministic limit is derived by utilizing the operator-valued free probability theory. Subsequently, an efficient projected gradient ascent (PGA) algorithm is proposed to optimize the transmit beamforming matrix with the aim of maximizing the weighted asymptotic MI. Numerical results validate that the derived closed-form expression matches well with the Monte Carlo simulation results and the proposed optimization algorithm is able to improve the weighted asymptotic MI significantly. We also illustrate the trade-off between asymptotic sensing and asymptotic communication MI.

Index Terms

Integrated sensing and communication, mutual information, beamforming design, free probability theory.

I. INTRODUCTION

The sixth generation (6G) wireless network has stimulated numerous innovative applications, such as smart cities and intelligent transportation. Toward this end, higher requirements of communication and sensing capabilities are raised for numerous nodes within the network. Due to the capability of enabling the dual functionalities of information transmission and target sensing with shared wireless resources, integrated sensing and communication (ISAC) has been regarded as a key enabler for the realization of 6G network [1].

As a promising approach to enhance the performances of ISAC systems, beamforming design has been investigated in numerous works adopting various communication and sensing performance metrics. In [2], the authors considered

Shanfeng Xu is with the School of Information and Electronics, Beijing Institute of Technology, Beijing 100081, China, and also with the China Academy of Electronics and Information Technology, Beijing 100041, China (e-mail: xushanfeng88@163.com).

Yanshuo Cheng, Siqiang Wang, Xinyi Wang, Zhong Zheng and Zesong Fei are with the School of Information and Electronics, Beijing Institute of Technology, Beijing 100081, China. (e-mails: chengyanshuobit@163.com, 3120205406@bit.edu.cn, bit_wangxy@163.com, zhong.zheng@bit.edu.cn, feizhong@bit.edu.cn)

transmit beam pattern and signal-to-interference-plus-noise (SINR) as sensing and communication performance metrics respectively. As a step further, due to its capability of characterizing the lower bound of parameter estimation, the Cramér-Rao Bound (CRB) has also been adopted as a sensing performance metric in ISAC systems [3].

In most existing works, the performance metrics for sensing and communications are diverse, resulting in difficulties in evaluating the trade-offs between sensing and communication performance. To facilitate ISAC beamforming design under unified performance metric, the authors in [4] proposed a Kullback-Leibler (KL) divergence based unified performance metric, and analyzed the error rate performance of communication users and detection performance for sensing targets. Based on this unified metric, the authors in [5] investigated constellation and beamforming design, and depicted the Pareto bound in terms of KL divergence as well as bit error rate and detection probability. Different from KL divergence, which concentrates on the reliability of data transmission, mutual information is closely related to the efficiency of transmission, and has also been utilized as the performance metric in ISAC systems. In [6], radar MI and communication channel capacity were formulated for ISAC systems. As a step further, in [7], OFDM-based ISAC waveform is designed with the aim of maximizing the weighted sum of the communication rates and the conditional radar MI. However, it should be noted that the aforementioned MI-oriented works are not conducted within the context of large dimensional antenna array, in which case In the case of large dimensional antenna array, perfect CSI becomes challenging to obtain, thereby affecting the accuracy of MI.

In this paper, we investigate the MI-oriented transmit beamforming design for a MIMO ISAC system, where an ISAC user equipment (UE) senses an extended target while simultaneously transmitting data to a base station (BS). Based on the channel state information (CSI) available at the UE, we formulate a transmit beamforming design problem with the aim of maximizing the weighted asymptotic MI. Applying the operator-valued free probability theory, we derive the closed-form expression of the weighted asymptotic MI and reformulate the beamforming design problem. Subsequently, based on the obtained closed-form expression, we propose an efficient projected gradient ascent (PGA) algorithm to solve the problem. Numerical results validate the accuracy of the derived expression, as well as the convergence and effectiveness of the proposed algorithm. In addition, the trade-off between sensing and communication MI is also depicted.

II. SYSTEM MODEL

A. Signal Model

We consider an ISAC system as shown in Fig. 1, where an ISAC UE is equipped with N_t transmit antennas and N_r receive antennas. The UE simultaneously transmits data to the BS equipped with N_u receive antennas and senses an extended target with L scatters uniformly distributed in the proximity of the center. The antennas at both UE and BS are assumed to be large dimensional antenna array. The transmit beamforming matrix of the UE is $\mathbf{W} \in \mathbb{C}^{N_t \times M}$. The data symbol matrix is denoted as $\mathbf{S} \in \mathbb{C}^{M \times N_s}$, where N_s denotes the number of signal samples and M denotes the number of data streams satisfying $M \leq N_t$. It is assumed that the signal vectors of \mathbf{S} are statistically orthogonal to each other, i.e., $\mathbb{E}[\mathbf{S}\mathbf{S}^\dagger] = \mathbf{I}_M$, with the notation $(\cdot)^\dagger$ denoting the conjugate transpose operation.

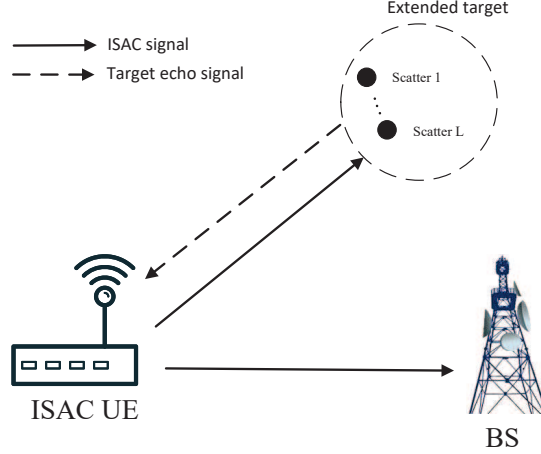


Fig. 1. Considered MIMO ISAC system.

The received signal at BS can be expressed as

$$\mathbf{Y}_c = \mathbf{H}_c \mathbf{W} \mathbf{S} + \mathbf{N}_C, \quad (1)$$

where \mathbf{H}_c is the channel between UE and BS, $\mathbf{N}_C \in \mathbb{C}^{N_u \times N_s}$ is the additive white Gaussian noise (AWGN) at the receiving antennas of BS and $\mathbf{N}_C \sim \mathcal{CN}(0, \sigma_c^2 \mathbf{I}_{N_s})$. The received echoes at the UE, $\mathbf{Y}_s \in \mathbb{C}^{N_r}$, can be expressed as

$$\mathbf{Y}_s = \sum_{l=1}^L \mathbf{G}_l \mathbf{W} \mathbf{S} + \mathbf{N}_S, \quad (2)$$

where $\mathbf{G}_l \in \mathbb{C}^{N_r \times N_t}$ is the round-trip channel matrix between the l -th scatterer and UE, $\mathbf{N}_S \in \mathbb{C}^{N_r \times N_s}$ is the AWGN at the receiving antennas of the UE and $\mathbf{N}_S \sim \mathcal{CN}(0, \sigma_s^2 \mathbf{I}_{N_s})$.

B. Channel Model

Due to the limitations of the Kronecker channel model in accurately representing the correlation between transceivers when scattering clusters are uniformly distributed, we employ the Weichselberger MIMO channel model [10], which captures the spatial correlation at both ends of the link and their mutual interdependence, for both radar sensing channel and the communication channel. The channels in (1) and (2) can be expressed as

$$\mathbf{H}_c = \overline{\mathbf{H}}_c + \tilde{\mathbf{H}}_c = \overline{\mathbf{H}}_c + \mathbf{U}(\mathbf{M} \odot \mathbf{P})\mathbf{V}^\dagger, \quad (3)$$

$$\mathbf{G}_l = \overline{\mathbf{G}}_l + \tilde{\mathbf{G}}_l = \overline{\mathbf{G}}_l + \mathbf{R}_l(\mathbf{N}_l \odot \mathbf{Q}_l)\mathbf{T}_l^\dagger, 1 \leq l \leq L, \quad (4)$$

where $\overline{\mathbf{H}}_c$ and $\overline{\mathbf{G}}_l$ are deterministic matrices which denote the line-of-sight (LoS) component of \mathbf{H}_c and \mathbf{G}_l . \mathbf{U} , \mathbf{V} , \mathbf{R}_l and \mathbf{T}_l are deterministic unitary matrices. \mathbf{M} and \mathbf{N}_l are deterministic nonnegative matrices which represent

the variance profiles of the random components $\tilde{\mathbf{H}}_c$ and $\tilde{\mathbf{G}}_l$ respectively. $\mathbf{P} \in \mathbb{C}^{N_u \times N_t}$ and $\mathbf{Q}_l \in \mathbb{C}^{N_r \times N_t}$ are complex Gaussian distributed with $[\mathbf{P}]_{i,j} \sim \mathcal{CN}(0, 1/N_t)$ and $[\mathbf{Q}_l]_{i,j} \sim \mathcal{CN}(0, 1/N_t)$.

C. Problem Formulation

From now on, for convenience of expression, we use $\tilde{I}_s(\sigma^2)$ and $\tilde{I}_c(\sigma^2)$ to denote $\tilde{I}_s(\sigma_s^2)$ and $\tilde{I}_c(\sigma_c^2)$, respectively. According to [11], the sensing MI can be expressed as

$$\begin{aligned} \tilde{I}_s(\sigma^2) &= \log \det \left(\mathbf{I}_{N_s} + \frac{1}{\sigma^2} \sum_{l=1}^L (\mathbf{S}^\dagger \mathbf{W}^\dagger \mathbf{G}_l^\dagger \mathbf{G}_l \mathbf{W} \mathbf{S}) \right) \\ &= \log \det \left(\mathbf{I}_{LN_r} + \frac{1}{\sigma^2} (\hat{\mathbf{G}} \mathbf{S} \mathbf{S}^\dagger \hat{\mathbf{G}}^\dagger) \right), \end{aligned} \quad (5)$$

where the matrix $\hat{\mathbf{G}}$ is defined as $\hat{\mathbf{G}} = [(\mathbf{G}_1 \mathbf{W})^\dagger, (\mathbf{G}_2 \mathbf{W})^\dagger, \dots, (\mathbf{G}_L \mathbf{W})^\dagger]^\dagger$. Based on the received signal at BS, the communication MI for the considered ISAC system can be expressed as [13]

$$\tilde{I}_c(\sigma^2) = \log \det \left(\mathbf{I}_{N_u} + \frac{1}{\sigma^2} \mathbf{H}_c \mathbf{Q} \mathbf{H}_c^\dagger \right), \quad (6)$$

where $\mathbf{Q} = \mathbf{W} \mathbf{W}^\dagger$. In order to achieve a balance between communication performance and sensing performance, we define a weighted MI as the performance metric for the proposed ISAC system, which is expressed as

$$\tilde{I}(\mathbf{W}) = \rho \tilde{I}_s(\sigma^2) + (1 - \rho) \tilde{I}_c(\sigma^2), \quad (7)$$

where ρ is a weighting factor that determines the weights of communication performance and sensing performance in the ISAC system. Furthermore, the transmit beamforming problem can be formulated as

$$(\mathbf{P1}) \max_{\mathbf{W}} \tilde{I}(\mathbf{W}) \quad (8a)$$

$$\text{s.t.} \quad \|\mathbf{W}\|_F^2 \leq P_t, \quad (8b)$$

where $\|\cdot\|_F^2$ denotes the Frobenius norm, (8b) is the transmit power constraint and P_t is the transmit power budget.

According to [12, Theorem 2], we have

$$\frac{1}{LN_r} \tilde{I}_s(\sigma^2) \xrightarrow[N_r \rightarrow \infty]{a.s.} I_s(\sigma^2) \quad (9)$$

$$\frac{1}{N_u} \tilde{I}_c(\sigma^2) \xrightarrow[N_u \rightarrow \infty]{a.s.} I_c(\sigma^2) \quad (10)$$

where the notation $\xrightarrow[N_r \rightarrow \infty]{a.s.}$ denotes the almost surely convergence as LN_r and N_t tend to infinity with the ratio LN_r/N_t fixed and $\xrightarrow[N_u \rightarrow \infty]{a.s.}$ denotes the almost surely convergence as N_u and N_t tend to infinity with the ratio N_u/N_t fixed. $I_s(\sigma^2)$ and $I_c(\sigma^2)$ are both deterministic, depending on the statistics of \mathbf{G}_l and \mathbf{H}_c , respectively. However, since the channel statistics are not perfectly known at UE, we aim to optimize the weighted asymptotic MI, which is defined as

$$I(\mathbf{W}) = \rho LN_r I_s(\sigma^2) + (1 - \rho) N_u I_c(\sigma^2), \quad (11)$$

Furthermore, the corresponding transmit beamforming problem can be formulated as:

$$(\mathbf{P2}) \max_{\mathbf{W}} I(\mathbf{W}) \quad (12a)$$

$$\text{s.t. } \|\mathbf{W}\|_F^2 \leq P_t. \quad (12b)$$

To solve this problem, we will derive the closed-form expression for the weighted asymptotic MI $I(\mathbf{W})$ in Section III.

III. PROBLEM REFORMULATION AND PROPOSED ALGORITHM

In this section, we reformulate Problem $(\mathbf{P1})$ and propose an efficient algorithm to solve the reformulated problem. Specially, in Section III-A, we first utilize the free probability theory and the linearization trick to derive the closed-form expression of the Cauchy transform. Based on this, we reformulate Problem $(\mathbf{P1})$ by deriving the closed-form expression for the weighted MI of the considered ISAC system. Finally, the PGA algorithm is proposed to solve the reformulated problem in Section III-B.

A. Problem Reformulation

Denote $\mathbf{B}_1 = \hat{\mathbf{G}}\mathbf{S}\mathbf{S}^\dagger\hat{\mathbf{G}}^\dagger$ and define the empirical cumulative distribution function (ECDF) of the B_1 's eigenvalues as

$$\tilde{F}_{\mathbf{B}_1}(x) = \frac{1}{LN_r} \sum_{i=1}^{LN_r} 1\{\lambda_i(\mathbf{B}_1) \leq x\}, \quad (13)$$

where $\lambda_1(\mathbf{B}_1), \dots, \lambda_{LN_r}(\mathbf{B}_1)$ are the eigenvalues of \mathbf{B}_1 and $1\{\cdot\}$ is the indicator function. Therefore, $\frac{1}{LN_r}\tilde{I}_s(\sigma^2)$ can be rewritten as

$$\begin{aligned} \frac{1}{LN_r}\tilde{I}_s(\sigma^2) &= \frac{1}{LN_r} \log \det \left(\mathbf{I}_{LN_r} + \frac{1}{\sigma^2} \mathbf{B}_1 \right), \\ &= \sum_{i=1}^{LN_r} \log \left(1 + \frac{1}{\sigma^2} \lambda_i(\mathbf{B}_1) \right), \\ &= \int_0^\infty \log \left(1 + \frac{1}{\sigma^2} x \right) d\tilde{F}_{\mathbf{B}_1}(x). \end{aligned} \quad (14)$$

For \mathbf{B}_1 , its resolvent $\tilde{\mathcal{G}}_{\mathbf{B}_1}(-z)$ and Cauchy transform $\mathcal{G}_{\mathbf{B}_1}(-z)$ for \mathbf{B}_1 are defined as

$$\tilde{\mathcal{G}}_{\mathbf{B}_1}(z) = \frac{1}{LN_r} \text{Tr}(z\mathbf{I} - \mathbf{B}_1)^{-1} = \int_0^\infty \frac{1}{z - \lambda} d\tilde{F}_{\mathbf{B}_1}, \quad (15)$$

$$\mathcal{G}_{\mathbf{B}_1}(z) = \frac{1}{LN_r} \mathbb{E} [\text{Tr}(z\mathbf{I} - \mathbf{B}_1)^{-1}] = \int_0^\infty \frac{1}{z - \lambda} dF_{\mathbf{B}_1}. \quad (16)$$

where $z = -\frac{1}{\sigma^2}$ and $F_{\mathbf{B}_1}$ is the cumulative distribution function (CDF) of the eigenvalues of \mathbf{B}_1 . Therefore, we have

$$\frac{1}{LN_r} \frac{d\tilde{I}_s(\sigma^2)}{dz} = -\frac{1}{z} - \tilde{\mathcal{G}}_{\mathbf{B}_1}(-z). \quad (17)$$

Applying the relationship between the Shannon transform $\mathcal{V}_{\mathbf{B}_1}(z)$ and the Cauchy transform $\mathcal{G}_{\mathbf{B}_1}(-z)$, the following equation holds

$$\frac{d\mathcal{V}_{\mathbf{B}_1}(z)}{dz} = -\frac{1}{z} - \mathcal{G}_{\mathbf{B}_1}(-z). \quad (18)$$

According to [16], the resolvent $\tilde{\mathcal{G}}_{\mathbf{B}_1}(-z)$ converges almost surely to the Cauchy transform $\mathcal{G}_{\mathbf{B}_1}(-z)$ for \mathbf{B}_1 . Therefore, we have

$$\frac{1}{LN_r} \tilde{I}_s(\sigma^2) \xrightarrow{LN_r \rightarrow \infty} \mathcal{V}_{\mathbf{B}_1}(z). \quad (19)$$

Since (9) holds, we can rewrite $I_s(\sigma^2)$ as

$$I_s(\sigma^2) = \mathcal{V}_{\mathbf{B}_1}(z). \quad (20)$$

Similarly, for the asymptotic communication MI, we have

$$I_c(\sigma^2) = \mathcal{V}_{\mathbf{B}_2}(z), \quad (21)$$

$$\frac{d\mathcal{V}_{\mathbf{B}_2}(z)}{dz} = -\frac{1}{z} - \mathcal{G}_{\mathbf{B}_2}(-z), \quad (22)$$

$$\mathcal{G}_{\mathbf{B}_2}(z) = \int_0^\infty \frac{1}{z-\lambda} dF_{\mathbf{B}_2}(\lambda) \quad (23)$$

where $\mathbf{B}_2 = \mathbf{H}_c \mathbf{Q} \mathbf{H}_c^\dagger$, $F_{\mathbf{B}_2}(\lambda)$ is CDF of \mathbf{B}_2 , $\mathcal{V}_{\mathbf{B}_2}(\sigma^2)$ is the Shannon transform of \mathbf{B}_2 and $\mathcal{G}_{\mathbf{B}_2}(z)$ is the Cauchy transform of \mathbf{B}_2 .

To obtain the closed-form expression of $\mathcal{G}_{\mathbf{B}_i}(z)$, free probability theory serves as a powerful analytical tool [15]. However, in the considered system, $\hat{\mathbf{G}}$ and \mathbf{S} are not free in the classic free probability aspect, resulting in difficulties in directly obtaining the Cauchy Transform for the product of $\hat{\mathbf{G}}$, \mathbf{S} , \mathbf{S}^\dagger and $\hat{\mathbf{G}}^\dagger$. To address this issue, the linearization trick will be adopted to embed the non-free matrices into a larger matrix, in which the deterministic parts and random parts are proved to be asymptotically free. Then the desired Cauchy transform can be obtained from the transformation of the operator-valued Cauchy transform for the embedded matrix. For the convenience of expression, we define $\overline{\mathbf{G}} = [(\overline{\mathbf{G}}_1 \mathbf{W})^T, (\overline{\mathbf{G}}_2 \mathbf{W})^T, \dots, (\overline{\mathbf{G}}_l \mathbf{W})^T]^T$ and $\overline{\mathbf{H}} = \overline{\mathbf{H}}_c \mathbf{W}$. Since I_c and I_s share a similar form, we only provide the detailed derivation of $\mathcal{G}_{\mathbf{B}_1}(z)$.

To obtain the closed-form of $\mathcal{G}_{\mathbf{B}_1}(z)$, we first apply the Anderson's linearization trick [15] to construct a block matrix of size $(LN_r + N_s + 2M) \times (LN_r + N_s + 2M)$ as

$$\mathbf{B}_L = \begin{bmatrix} \mathbf{0}_{LN_r \times LN_r} & \mathbf{0}_{LN_r \times M} & \mathbf{0}_{LN_r \times N_s} & \hat{\mathbf{G}} \\ \mathbf{0}_{M \times LN_r} & \mathbf{0}_{M \times M} & \mathbf{S} & -\mathbf{I}_M \\ \mathbf{0}_{N_s \times LN_r} & \mathbf{S}^\dagger & -\mathbf{I}_{N_s} & \mathbf{0}_{N_s \times M} \\ \hat{\mathbf{G}}^\dagger & -\mathbf{I}_M & \mathbf{0}_{M \times N_s} & \mathbf{0}_{M \times M} \end{bmatrix}. \quad (24)$$

The operator-valued Cauchy transform $\mathcal{G}_{\mathbf{B}_L}^{\mathcal{D}}$ of \mathbf{B}_L [15] is given by

$$\mathcal{G}_{\mathbf{B}_L}^{\mathcal{D}}(\mathbf{\Lambda}(z)) = \mathbb{E}_{\mathcal{D}} \left[(\mathbf{\Lambda}(z) - \mathbf{B}_L)^{-1} \right], \quad (25)$$

where $\mathbb{E}_{\mathcal{D}}[\mathbf{X}]$ is defined as

$$\mathbb{E}_{\mathcal{D}}[\mathbf{X}] = \begin{bmatrix} \mathbb{E}[\mathbf{X}_1] & & & \\ \text{---} & \mathbb{E}[\mathbf{X}_2] & & \\ \text{---} & \text{---} & \mathbb{E}[\mathbf{X}_3] & \\ \text{---} & \text{---} & \text{---} & \mathbb{E}[\mathbf{X}_4] \end{bmatrix}, \quad (26)$$

where $\mathbf{X}_1 = \{\mathbf{X}\}_1^{LN_r}$, $\mathbf{X}_2 = \{\mathbf{X}\}_{LN_r+1}^{LN_r+M}$, $\mathbf{X}_3 = \{\mathbf{X}\}_{LN_r+M+1}^{LN_r+M+N_s}$, $\mathbf{X}_4 = \{\mathbf{X}\}_{LN_r+M+N_s+1}^{LN_r+2M+N_s}$, with the notation $\{\mathbf{A}\}_a^b$ denoting the submatrix of \mathbf{A} containing the rows and columns with indices from a to b , i.e., $[\{\mathbf{A}\}_a^b]_{i,j} = [\mathbf{A}]_{i+a-1,j+a-1}$ for $1 \leq i, j \leq b-a+1$, where the notation $[\mathbf{A}]_{i,j}$ is the element in the i -th row and j -th column of matrix \mathbf{A} . The matrix function $\Lambda(z)$ is defined as

$$\Lambda(z) = \begin{bmatrix} z\mathbf{I}_{LN_r} & \mathbf{0}_{LN_r \times (N_s+2M)} \\ \mathbf{0}_{(N_s+2M) \times LN_r} & \mathbf{0}_{(N_s+2M) \times (N_s+2M)} \end{bmatrix}. \quad (27)$$

Then $\mathcal{G}_{\mathbf{B}_1}(z)$ is given by

$$\mathcal{G}_{\mathbf{B}_1}(z) = \frac{1}{LN_r} \text{Tr} \left(\{\mathcal{G}_{\mathbf{B}_L}^{\mathcal{D}}(\Lambda(z))\}^{(1,1)} \right), \quad (28)$$

where $\{\cdot\}^{(1,1)}$ represents the upper-left $LN_r \times LN_r$ matrix block and the operator $\text{Tr}(\cdot)$ represents the trace of the matrix. It can be observed that \mathbf{B}_L shares a similar structure with the matrix \mathbf{L} proposed in [17, Prop. 2], which inspires us to use the method in [17]. Specifically, the Cauchy transform $\mathcal{G}_{\mathbf{B}_1}(z)$ can be obtained with the following proposition.

Proposition 1. *The Cauchy transform of \mathbf{B}_1 , with $z \in \mathbb{C}^+$, is given by*

$$\mathcal{G}_{\mathbf{B}_1}(z) = \frac{1}{LN_r} \text{Tr} [\mathcal{G}_{\tilde{\mathbf{C}}}(z)], \quad (29)$$

where $\mathcal{G}_{\tilde{\mathbf{C}}}(z)$ satisfies the following equations

$$\mathcal{G}_{\tilde{\mathbf{C}}}(z) = \left(\tilde{\Psi}(z) - \overline{\mathbf{G}}\mathbf{\Pi}^{-1}\overline{\mathbf{G}}^\dagger \right)^{-1}, \quad (30)$$

$$\mathbf{\Pi} = \Psi(z) - \tilde{\Phi}(z)^{-1}, \quad (31)$$

where the matrices $\tilde{\Psi}(z)$, $\Psi(z)$, $\tilde{\Phi}(z)$, $\Phi(z)$ are respectively denoted as

$$\tilde{\Psi}(z) = z\mathbf{I}_{LN_r} - \text{diag} \{ \tilde{\eta}_1(\mathcal{G}_{\mathbf{C}}(z)), \dots, \tilde{\eta}_L(\mathcal{G}_{\mathbf{C}}(z)) \}, \quad (32)$$

$$\Psi(z) = - \sum_{l=1}^L \eta_l(\mathcal{G}_{\tilde{\mathbf{C}}_l}(z)), \quad (33)$$

$$\tilde{\Phi}(z) = -\tilde{\zeta}(\mathcal{G}_{\tilde{\mathbf{D}}}(z)), \quad (34)$$

$$\Phi(z) = \mathbf{I}_{N_s} - \zeta(\mathcal{G}_{\mathbf{D}}(z)), \quad (35)$$

where the notation $\text{diag}(\mathbf{A}, \dots, \mathbf{B})$ represents the diagonal block matrix constructed by $\mathbf{A}, \dots, \mathbf{B}$ matrices and

$\eta_l(\tilde{\mathbf{C}})$, $\tilde{\eta}_l(\mathbf{C})$, $\zeta(\mathbf{D})$, $\tilde{\zeta}(\tilde{\mathbf{D}})$ are the parameterized one-sided correlation matrices, which are shown as (57), (58), (65) and (66) in Appendix A. The matrices $\mathcal{G}_{\mathbf{C}}(z)$, $\mathcal{G}_{\tilde{\mathbf{D}}}(z)$, $\mathcal{G}_{\mathbf{D}}(z)$, and $\mathcal{G}_{\tilde{\mathbf{C}}_l}(z)$ are defined as

$$\mathcal{G}_{\mathbf{C}}(z) = \left(\Psi(z) - \bar{\mathbf{G}}^\dagger \tilde{\Psi}(z)^{-1} \bar{\mathbf{G}}^\dagger - \tilde{\Phi}(z)^{-1} \right)^{-1}, \quad (36)$$

$$\mathcal{G}_{\tilde{\mathbf{D}}}(z) = \Phi(z)^{-1}, \quad (37)$$

$$\mathcal{G}_{\mathbf{D}}(z) = \left(\tilde{\Phi}(z) - \left(\Psi(z) - \bar{\mathbf{G}}^\dagger \tilde{\Psi}(z) \bar{\mathbf{G}} \right)^{-1} \right)^{-1}, \quad (38)$$

$$\mathcal{G}_{\tilde{\mathbf{C}}_l}(z) = \{ \mathcal{G}_{\tilde{\mathbf{C}}}(z) \}_{1+(l-1)N_r}^{lN_r}. \quad (39)$$

Proof. The proof of this Proposition 1 is similar to the method presented in [17, Prop. 2]. Therefore we provide a brief outline of the proof. First, we prove that the deterministic and random components of the linearized matrix are free. Then, by applying the subordination formula, we derive the equation for the operator-valued Cauchy transform. Finally, using the matrix inversion formula, we decompose the operator-valued Cauchy transform, thereby obtaining the above expressions. \square

Based on the closed-form expression of the Cauchy transformation $\mathcal{G}_{\mathbf{B}_1}(z)$, we can derive the closed-form expression of the Shannon transform $\mathcal{V}_{\mathbf{B}_1}(z)$ in the following proposition.

Proposition 2. *The Shannon transform $\mathcal{V}_{\mathbf{B}_1}(z)$, with $z \in \mathbb{C}^+$, is given by*

$$\begin{aligned} \mathcal{V}_{\mathbf{B}_1}(z) &= \frac{1}{LN_r} \log \det \left(\frac{\tilde{\Psi}(-z)}{-z} \right) + \frac{1}{LN_r} \log \det \left(\Psi(-z) - \bar{\mathbf{G}}^\dagger \tilde{\Psi}(-z)^{-1} \bar{\mathbf{G}}^\dagger - \tilde{\Phi}(-z)^{-1} \right) \\ &+ \frac{1}{LN_r} \log \det \left(\tilde{\Phi}(-z) \right) + \frac{1}{LN_r} \text{Tr} \left(\mathcal{G}_{\tilde{\mathbf{C}}}(-z) \left(-z \mathbf{I}_{LN_r} - \tilde{\Psi}(-z) \right) \right), \\ &+ \frac{1}{LN_r} \text{Tr} \left(\mathcal{G}_{\tilde{\mathbf{D}}}(-z) \zeta \right) + \frac{1}{LN_r} \log \det \left(\Phi(-z) \right) \end{aligned} \quad (40)$$

where $\tilde{\Psi}(-z)$, $\Psi(-z)$, $\tilde{\Phi}(-z)$, $\mathcal{G}_{\tilde{\mathbf{D}}}(-z)$, $\mathcal{G}_{\mathbf{D}}(-z)$, and $\mathcal{G}_{\tilde{\mathbf{C}}}(-z)$ are given by (30)-(35) in Proposition 1.

Proof. The proof of Proposition 2 is given in Appendix A. \square

Similarly, the Cauchy transform $\mathcal{G}_{\mathbf{B}_2}(z)$ of \mathbf{B}_2 and the Shannon transform $\mathcal{V}_{\mathbf{B}_2}(z)$, with $z \in \mathbb{C}^+$, are given by

$$\mathcal{G}_{\mathbf{B}_2}(z) = \frac{1}{N_u} \text{Tr} \left[\mathcal{G}_{\tilde{\mathbf{E}}}(z) \right], \quad (41)$$

$$\begin{aligned} \mathcal{V}_{\mathbf{B}_2}(z) &= \frac{1}{N_u} \log \det \left(\frac{\tilde{\Omega}(-z)}{-z} \right) + \frac{1}{N_u} \text{Tr} \left(\mathcal{G}_{\tilde{\mathbf{E}}}(-z) \tilde{\tau} \right) \\ &- \frac{1}{N_u} \log \det \left(\mathcal{G}_{\mathbf{E}}(-z) \right), \end{aligned} \quad (42)$$

where $\eta_l(\tilde{\mathbf{C}})$, $\tilde{\eta}_l(\mathbf{C})$, $\tau(\mathbf{E})$, $\tilde{\tau}(\tilde{\mathbf{E}})$ are the parameterized one-sided correlation matrices, which are shown as (57),

(58), (61) and (62) in Appendix A. The matrices $\mathcal{G}_{\tilde{\mathbf{E}}}(z)$, $\mathcal{G}_{\mathbf{E}}(z)$, $\tilde{\mathbf{\Omega}}(z)$ and $\mathbf{\Omega}(z)$ satisfy the following equations

$$\mathcal{G}_{\tilde{\mathbf{E}}}(z) = \left(\tilde{\mathbf{\Omega}}(z) - \bar{\mathbf{H}}\mathbf{\Omega}(z)^{-1}\bar{\mathbf{H}}^\dagger \right)^{-1}, \quad (43)$$

$$\mathcal{G}_{\mathbf{E}}(z) = \left(\mathbf{\Omega}(z) - \bar{\mathbf{H}}^\dagger \tilde{\mathbf{\Omega}}(z)^{-1}\bar{\mathbf{H}} \right)^{-1}, \quad (44)$$

$$\tilde{\mathbf{\Omega}}(z) = z\mathbf{I}_{N_u} - \tilde{\tau}(\mathcal{G}_{\mathbf{E}}(z)), \quad (45)$$

$$\mathbf{\Omega}(z) = 1 - \tau(\mathcal{G}_{\tilde{\mathbf{E}}}(z)). \quad (46)$$

From now on, for convenience of expression, we refer to the asymptotic sensing MI, asymptotic communication MI and weighted asymptotic MI as the sensing MI, communication MI and weighted MI, respectively. Then the sensing MI, the communication MI and the weighted MI can be rewritten as

$$I_s(z, \mathbf{W}) = LN_r \mathcal{V}_{\mathbf{B}_1}(\sigma^2), \quad (47)$$

$$I_c(z, \mathbf{W}) = N_u \mathcal{V}_{\mathbf{B}_2}(\sigma^2), \quad (48)$$

$$I(z, \mathbf{W}) = \rho I_s(z, \mathbf{W}) + (1 - \rho) I_c(z, \mathbf{W}). \quad (49)$$

Consequently, we reformulate the problem **(P2)** as

$$\text{(P3)} \quad \max_{\mathbf{W}} I(z, \mathbf{W}) \quad (50a)$$

$$\text{s.t.} \quad (8b). \quad (50b)$$

B. Proposed PGA Algorithm

In order to solve the problem **(P3)**, we propose the PGA algorithm. Firstly, we calculate the gradient of the weighted MI in (49). Then the updated beamforming matrix at the $(i + 1)$ -th iteration is updated as

$$\tilde{\mathbf{W}}^{[i+1]} = \mathbf{W}^{[i]} + \lambda \nabla g_{\mathbf{W}} \left(\mathbf{W}^{[i]} \right), \quad (51)$$

where $\mathbf{W}^{[i]}$ denotes the beamforming matrix at the i -th iteration, λ denotes the step size, and the element of gradient $\nabla g_{\mathbf{W}}$ of $I(z, \mathbf{W})$ is given by (56), where $\mathbf{E}_{i,j}$ is a matrix whose elements satisfy

$$[\mathbf{E}_{i,j}]_{s,t} = \begin{cases} 1, & \text{if } s = i \text{ and } t = j, \\ 0, & \text{otherwise.} \end{cases} \quad (52)$$

To satisfy the transmit power constraint (8b), the solution $\tilde{\mathbf{W}}^{[i+1]}$ is then projected onto the feasible region. The obtained solution at the $(i + 1)$ -th iteration is given by

$$\mathbf{W}^{[i+1]} = \text{Proj}_{\mathcal{W}} \left(\tilde{\mathbf{W}}^{[i+1]} \right), \quad (53)$$

(55)

$$\begin{aligned}
[\nabla g_{\mathbf{W}}]_{i,j} = & \rho \text{Tr} \left(\left(-\Psi + \mathbf{W}^\dagger \bar{\mathbf{G}} \tilde{\Psi}^{-1} \bar{\mathbf{G}} \mathbf{W} + \tilde{\Phi}^{-1} \right)^{-1} \mathbf{E}_{i,j}^\dagger \bar{\mathbf{G}}^\dagger \tilde{\Psi}^{-1} \bar{\mathbf{G}} \mathbf{W} \right) \\
& + (\rho - 1) \text{Tr} \left(\left(\Omega - \mathbf{W}^\dagger \bar{\mathbf{H}}^\dagger \tilde{\Omega}^{-1} \bar{\mathbf{H}} \mathbf{W} \right)^{-1} \mathbf{E}_{i,j}^\dagger \bar{\mathbf{H}}^\dagger \tilde{\Omega}^{-1} \bar{\mathbf{H}} \mathbf{W} \right),
\end{aligned} \tag{56}$$

where the projection operator is given as

$$\text{Proj}_{\mathcal{W}} = \begin{cases} \mathbf{W}, & \text{if } \|\mathbf{W}\|_F^2 \leq P_t, \\ \sqrt{P_t} \frac{\mathbf{W}}{\|\mathbf{W}\|_F}, & \text{otherwise.} \end{cases} \tag{54}$$

The detailed algorithm is presented in Algorithm 1.

Algorithm 1 PGA algorithm for beamforming matrix design

initialize: Set the convergence criterion ε , $i = 0$, and randomly generate the beamforming matrix $\mathbf{W}^{[0]}$. Calculate $I^{[0]}$ based on (49).

repeat

 Update $\mathbf{W}^{[i+1]}$ based on (53).

 Calculate $I^{[i+1]}$ based on (49).

$i = i + 1$.

until $|I^{[i]} - I^{[i-1]}| \leq \varepsilon$.

output Optimal beamforming matrix \mathbf{W} .

IV. NUMERICAL RESULTS

In this section, we provide numerical results to verify the accuracy of the derived closed-form weighted MI expression and the effectiveness of the proposed PGA algorithm. For the channel settings, the deterministic components are modeled as the direct links between uniform planar arrays (UPA) equipped at both the transmitter and the receiver. In addition, statistical characteristics parameters of the channel including the deterministic unitary matrices \mathbf{U} , \mathbf{V} , \mathbf{R}_t and \mathbf{T}_t , as well as the variance matrices \mathbf{M} and \mathbf{N}_t , are generated randomly but fixed in each Monte Carlo simulation. Unless otherwise stated, the number of scatters, data streams and signal samples are set as $L = 2$, $M = N_u$, and $N_s = M$, respectively. In addition, the transmit power budget is set as $P_t = N_t$. It should be noted that since the radar detection link distance is typically longer than the communication link distance to UE, without loss of generality, we assume that the signal-noise-ratio (SNR) at BS is 20 dB higher than the SNR at UE. Besides, the SNR mentioned in this section refers to the SNR at BS. Furthermore, the beamforming matrix is set as $\mathbf{W} = \sqrt{P_t/M} \mathbf{I}_M$ without optimization. All simulation results are generated by averaging over 10^4 channel realizations.

We first verify the accuracy of the obtained closed-form MI expression for communication MI and sensing MI without optimization in Fig. 3. The number of antennas are $N_t = N_r = N_u = 16$. The solid lines represent theoretical results calculated by the communication MI expression and sensing MI expression, where the markers

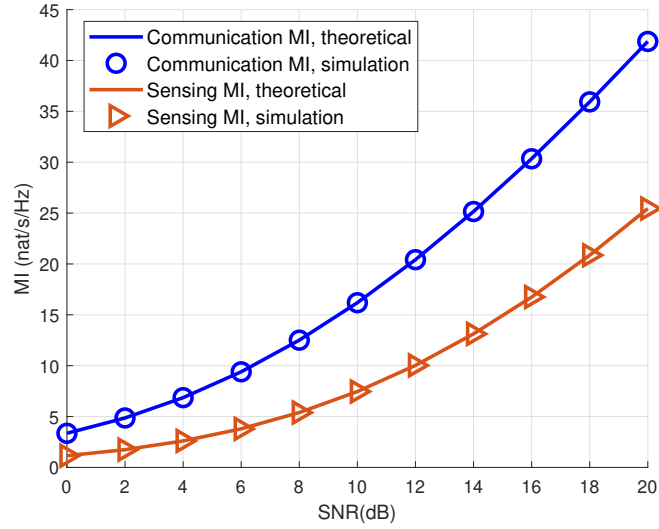


Fig. 2. Communication MI and sensing MI versus SNR.

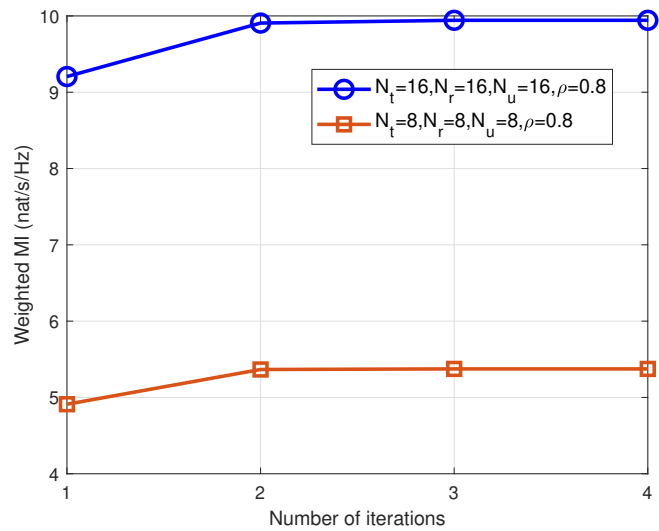


Fig. 3. Weighted MI versus the number of iterations, where $\rho = 0.8$.

represent corresponding Monte Carlo simulation results. It can be observed that the theoretical analyses match the simulation results excellently, verifying the accuracy of our derived results.

Subsequently, the convergence of the proposed PGA algorithm under different numbers of antennas is plotted in Fig. 3. The weighting factor and the SNR are set as $\rho = 0.8$ and 10 dB respectively. It can be observed that the weighted MI increases with the number of antennas. This is because a larger number of antennas provides higher diversity gain and greater design degrees of freedom (DoFs). In addition, the weighted MI increases with the iterations and converges within 3 iterations, demonstrating the fast convergence of the proposed PGA algorithm.

To demonstrate the effectiveness of the proposed optimization algorithm, we show the optimized weighted MI

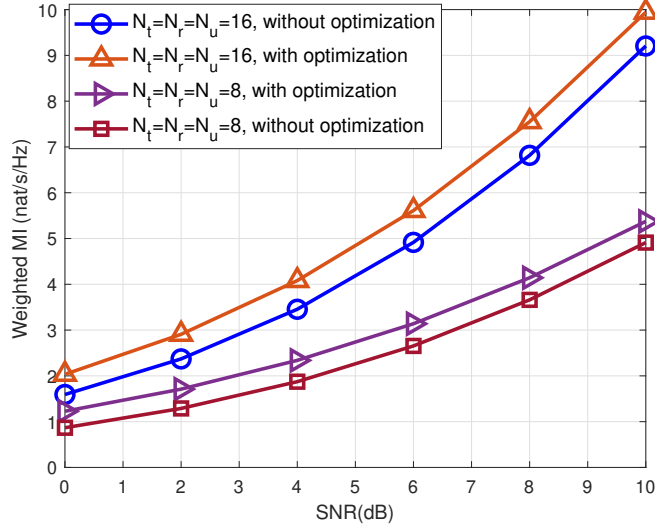


Fig. 4. Weighted MI versus SNR with different schemes, where $\rho = 0.8$.

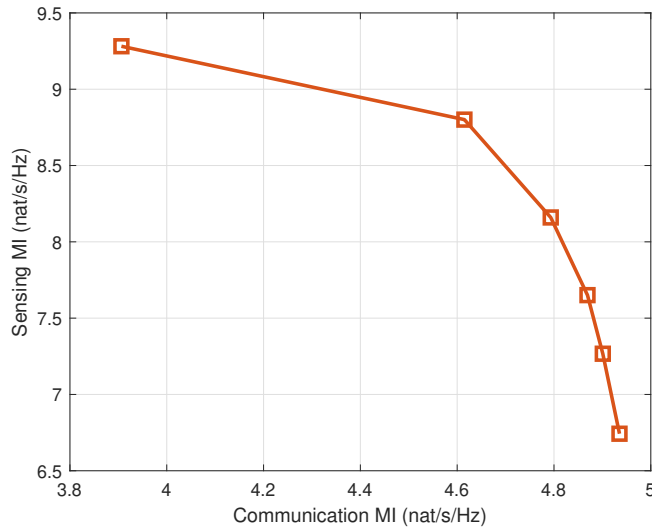


Fig. 5. Sensing MI versus Communication MI.

with different numbers of antennas for the considered system in Fig. 5. The weighting factor is set as $\rho = 0.8$. It can be observed that with the same SNR, the proposed PGA algorithm can improve the weighted MI.

To further depict the trade-off between sensing and communication MI, we show the optimized weighted MI with weighting factors ρ ranging from 0 to 1 in Fig. 5. The number of antennas and the SNR are set as $N_t = N_r = N_u = 8$ and 10 dB, respectively. As the weighting factor increases, the ISAC system places greater emphasis on sensing performance, and conversely, prioritizes communication performance when the weighting factor decreases.

V. CONCLUSIONS

In this paper, we investigated the beamforming design for a practical MIMO ISAC system. To derive the closed-form expression of the weighted MI for the considered system, we resorted to the operator-valued free probability. Based on the closed-form expression, we proposed the PGA algorithm to design the transmit beamforming matrix for maximizing the weighted MI. Simulation results verified the accuracy of the derived closed-form expression and the effectiveness of the proposed algorithm.

APPENDIX

We define the parameterized one-sided correlation matrices of \mathbf{G}_l as

$$\eta_l(\tilde{\mathbf{C}}) = \mathbb{E}[\tilde{\mathbf{G}}_l^\dagger \tilde{\mathbf{C}} \tilde{\mathbf{G}}_l] = \frac{1}{N_t} \mathbf{T}_l \mathbf{\Pi}_l(\tilde{\mathbf{C}}) \mathbf{T}_l^\dagger, 1 \leq l \leq L, \quad (57)$$

$$\tilde{\eta}_l(\mathbf{C}) = \mathbb{E}[\tilde{\mathbf{G}}_l \mathbf{C} \tilde{\mathbf{G}}_l^\dagger] = \frac{1}{N_t} \mathbf{R}_l \tilde{\mathbf{\Pi}}_l(\mathbf{C}) \mathbf{R}_l^\dagger, 1 \leq l \leq L, \quad (58)$$

where $\tilde{\mathbf{C}} \in \mathbb{C}^{N_t \times N_t}$ and $\mathbf{C}_l \in \mathbb{C}^{N_r \times N_r}$ are any Hermitian matrices, $\mathbf{\Pi}_l(\tilde{\mathbf{C}})$ and $\tilde{\mathbf{\Pi}}_l(\mathbf{C})$ are diagonal matrices with the entries given by

$$\left[\mathbf{\Pi}_l(\tilde{\mathbf{C}}) \right]_{i,i} = \sum_{j=1}^{N_r} ([\mathbf{N}_l]_{j,i})^2 \left[\mathbf{R}_l^\dagger \tilde{\mathbf{C}} \mathbf{R}_l \right]_{j,j}, 1 \leq i \leq N_t, \quad (59)$$

$$\left[\tilde{\mathbf{\Pi}}_l(\mathbf{C}) \right]_{i,i} = \sum_{j=1}^{N_t} ([\mathbf{N}_l]_{i,j})^2 \left[\mathbf{T}_l^\dagger \mathbf{C} \mathbf{T}_l \right]_{j,j}, 1 \leq i \leq N_r. \quad (60)$$

Similarly, the parameterized one-sided correlation matrices of \mathbf{H}_c , are defined as

$$\tau(\mathbf{E}) = \mathbb{E}[\tilde{\mathbf{H}}_c^\dagger \mathbf{E} \tilde{\mathbf{H}}_c] = \frac{1}{N_t} \mathbf{V} \mathbf{\Sigma}(\mathbf{E}) \mathbf{V}^\dagger, \quad (61)$$

$$\tilde{\tau}(\tilde{\mathbf{E}}) = \mathbb{E}[\tilde{\mathbf{H}}_c \tilde{\mathbf{E}} \tilde{\mathbf{H}}_c^\dagger] = \frac{1}{N_t} \mathbf{U} \tilde{\mathbf{\Sigma}}(\tilde{\mathbf{E}}) \mathbf{U}^\dagger, \quad (62)$$

where $\tilde{\mathbf{E}} \in \mathbb{E}^{N_t \times N_t}$ and $\mathbf{E} \in \mathbb{C}^{N_u \times N_u}$ are arbitrary Hermitian matrices. $\mathbf{\Sigma}(\mathbf{E})$ and $\tilde{\mathbf{\Sigma}}(\tilde{\mathbf{E}})$ are diagonal matrices with the entries given by

$$\left[\mathbf{\Sigma}(\mathbf{E}) \right]_{i,i} = \sum_{j=1}^{N_u} ([\mathbf{M}]_{j,i})^2 \left[\mathbf{U}^\dagger \mathbf{D} \mathbf{U} \right]_{j,j}, \quad (63)$$

$$\left[\tilde{\mathbf{\Sigma}}(\tilde{\mathbf{E}}) \right]_{i,i} = \sum_{j=1}^{N_t} ([\mathbf{M}]_{i,j})^2 \left[\mathbf{V}^\dagger \tilde{\mathbf{E}} \mathbf{V} \right]_{j,j}. \quad (64)$$

The parameterized one-sided correlation matrices of \mathbf{S} are

$$\zeta(\mathbf{D}) = \mathbb{E}[\mathbf{S}^\dagger \mathbf{D} \mathbf{S}] = \frac{1}{N_s} \text{Tr}(\mathbf{D}) \mathbf{I}_{N_s}, \quad (65)$$

$$\tilde{\zeta}(\tilde{\mathbf{D}}) = \mathbb{E}[\mathbf{S} \tilde{\mathbf{D}} \mathbf{S}^\dagger] = \frac{1}{N_s} \text{Tr}(\tilde{\mathbf{D}}) \mathbf{I}_M, \quad (66)$$

where $\tilde{\mathbf{D}} \in \mathbb{C}^{N_s \times N_s}$ and $\mathbf{D} \in \mathbb{C}^{M \times M}$ are any Hermitian matrices. To prove the Proposition 2, we need to prove that (17) holds with the $\mathcal{V}_{\mathbf{B}_1}(z)$ given in (40). The partial derivative of $\mathcal{V}_{\mathbf{B}}(z)$ with respect to z is given by

$$\begin{aligned} \frac{d}{dz} \mathcal{V}_{\mathbf{B}_1}(z) &= \frac{1}{LN_r} \frac{d}{dz} \log \det \left(\frac{\tilde{\Psi}}{-z} \right) + \frac{1}{LN_r} \frac{d}{dz} \log \det \left(\Psi - \bar{\mathbf{G}}^\dagger \tilde{\Psi}^{-1} \bar{\mathbf{G}}^\dagger - \tilde{\Phi}^{-1} \right), \\ &+ \frac{1}{LN_r} \frac{d}{dz} \log \det \left(\tilde{\Phi} \right) + \frac{1}{LN_r} \frac{d}{dz} \text{Tr} \left(\mathcal{G}_{\tilde{\mathbf{C}}} \left(-z \mathbf{I}_{LN_r} - \tilde{\Psi} \right) \right), \\ &+ \frac{1}{LN_r} \frac{d}{dz} \text{Tr} \left(\mathcal{G}_{\tilde{\mathbf{D}}} \zeta \right) + \frac{1}{LN_r} \frac{d}{dz} \log \det \left(\Phi \right) \end{aligned} \quad (67)$$

where notation $(-z)$ are omitted for convenience. For a matrix function $\mathbf{K}(z)$, the following equations hold:

$$\frac{d}{dz} \log \det \mathbf{K}(z) = \text{Tr} \left(\mathbf{K}(z)^{-1} \frac{d\mathbf{K}(z)}{dz} \right), \quad (68)$$

$$\text{Tr} \left(\frac{d\mathbf{K}(z)^{-1}}{dz} \right) = -\text{Tr} \left(\mathbf{K}(z)^{-1} \frac{d\mathbf{K}(z)}{dz} \mathbf{K}(z)^{-1} \right). \quad (69)$$

According to [18, Lemma1], the following equations hold:

$$\text{Tr}(\mathbf{A}_1 \eta_l(\mathbf{A}_2)) = \text{Tr}(\mathbf{A}_2 \tilde{\eta}_l(\mathbf{A}_1)), 1 \leq l \leq L, \quad (70)$$

$$\text{Tr}(\mathbf{B}_1 \zeta(\mathbf{B}_2)) = \text{Tr}(\mathbf{B}_2 \tilde{\zeta}(\mathbf{B}_1)). \quad (71)$$

Then we will simplify the terms on the right-hand side of equation (67) based on (68), (69), (70) and (71).

For the first term of (67), we can obtain

$$\begin{aligned} \frac{d}{dz} \log \det \left(\frac{\tilde{\Psi}}{-z} \right) &= \text{Tr} \left(\left(\frac{\tilde{\Psi}}{-z} \right)^{-1} \frac{d \left(\frac{\tilde{\Psi}}{-z} \right)}{dz} \right) \\ &= \text{Tr} \left(-\frac{1}{z} \mathbf{I} + \tilde{\Psi}^{-1} \frac{d\tilde{\Psi}}{dz} \right) \\ &= -\frac{LN_r}{z} + \text{Tr} \left(\tilde{\Psi}^{-1} \frac{d\tilde{\Psi}}{dz} \right). \end{aligned} \quad (72)$$

For the second term, the third term and the last term in (67), we can get

$$\frac{d}{dz} \log \det \left(-\tilde{\Phi}^{-1} + \Delta \right) = \text{Tr} \left(\left(-\tilde{\Phi}^{-1} + \Delta \right)^{-1} \frac{d \left(-\tilde{\Phi}^{-1} + \Delta \right)}{dz} \right), \quad (73)$$

$$\frac{d}{dz} \log \det \left(\tilde{\Phi} \right) = \text{Tr} \left(\tilde{\Phi}^{-1} \frac{d\tilde{\Phi}}{dz} \right), \quad (74)$$

$$\frac{d}{dz} \log \det \left(\Phi \right) = \text{Tr} \left(\Phi^{-1} \frac{d\Phi}{dz} \right), \quad (75)$$

where Δ is denoted as $\Delta = \Psi - \bar{\mathbf{G}}^\dagger \tilde{\Psi}^{-1} \bar{\mathbf{G}}^\dagger$. Therefore $\mathcal{G}_{\tilde{\mathbf{C}}}$ and $\mathcal{G}_{\tilde{\mathbf{D}}}$ can be expressed as

$$\mathcal{G}_{\tilde{\mathbf{C}}} = \left(\Delta - \tilde{\Phi}^{-1} \right)^{-1}, \quad (76)$$

$$\mathcal{G}_{\tilde{\mathbf{D}}} = \left(\tilde{\Phi}(z) - \Delta^{-1} \right)^{-1}. \quad (77)$$

By applying (70), (71) and the Woodbury identity, the forth and the fifth term can be expressed as

$$\begin{aligned}
& \frac{d}{dz} \text{Tr} \left(\mathcal{G}_{\tilde{\mathbf{C}}} \left(-z \mathbf{I}_{LNr} - \tilde{\Psi} \right) \right) \\
&= \text{Tr} \left(\mathcal{G}_{\tilde{\mathbf{C}}} \frac{d \left(-z \mathbf{I}_{LNr} - \tilde{\Psi} \right)}{dz} \right) + \text{Tr} \left(\text{diag} \{ \tilde{\eta}_1(\mathcal{G}_{\mathbf{C}}), \dots, \tilde{\eta}_L(\mathcal{G}_{\mathbf{C}}) \} \frac{d \mathcal{G}_{\tilde{\mathbf{C}}}}{dz} \right) \\
&= \text{Tr} \left(\mathcal{G}_{\tilde{\mathbf{C}}} \frac{d \left(-z \mathbf{I}_{LNr} - \tilde{\Psi} \right)}{dz} \right) + \text{Tr} \left(\mathcal{G}_{\mathbf{C}} \frac{d \left(\sum_{l=1}^L \eta_l(\mathcal{G}_{\tilde{\mathbf{C}}_l}) \right)}{dz} \right) \\
&= -\text{Tr}(\mathcal{G}_{\tilde{\mathbf{C}}}) - \text{Tr} \left(\mathcal{G}_{\tilde{\mathbf{C}}} \frac{d \tilde{\Psi}}{dz} \right) - \text{Tr} \left(\mathcal{G}_{\mathbf{C}} \frac{d \Psi}{dz} \right) \\
&= -\text{Tr}(\mathcal{G}_{\tilde{\mathbf{C}}}) - \text{Tr} \left(\left(\tilde{\Psi}(z)^{-1} + \tilde{\Psi}(z)^{-1} \bar{\mathbf{G}} \mathcal{G}_{\mathbf{C}} \bar{\mathbf{G}}^\dagger \tilde{\Psi}(z)^{-1} \right) \frac{d \tilde{\Psi}}{dz} \right) - \text{Tr} \left(\mathcal{G}_{\mathbf{C}} \frac{d \Psi}{dz} \right) \\
&= -\text{Tr}(\mathcal{G}_{\tilde{\mathbf{C}}}) - \text{Tr} \left(\tilde{\Psi}^{-1} \frac{d \tilde{\Psi}}{dz} \right) + \text{Tr} \left(\mathcal{G}_{\mathbf{C}} \frac{d \left(\bar{\mathbf{G}}^\dagger \tilde{\Psi} \bar{\mathbf{G}} \right)}{dz} \right) - \text{Tr} \left(\mathcal{G}_{\mathbf{C}} \frac{d \Psi}{dz} \right), \tag{78}
\end{aligned}$$

$$\begin{aligned}
& \frac{d \text{Tr}(\mathcal{G}_{\tilde{\mathbf{D}}} \zeta)}{dz} \\
&= \text{Tr} \left(\mathcal{G}_{\tilde{\mathbf{D}}} \frac{d \zeta}{dz} \right) + \text{Tr} \left(\zeta \frac{d \mathcal{G}_{\tilde{\mathbf{D}}}}{dz} \right) \\
&= \text{Tr} \left(\mathcal{G}_{\tilde{\mathbf{D}}} \frac{d(\mathbf{I} - \Phi)}{dz} \right) + \text{Tr} \left(\mathcal{G}_{\mathbf{D}} \frac{d \tilde{\zeta}}{dz} \right) \\
&= -\text{Tr} \left(\mathcal{G}_{\tilde{\mathbf{D}}} \frac{d \Phi}{dz} \right) - \text{Tr} \left(\mathcal{G}_{\mathbf{D}} \frac{d \tilde{\Phi}}{dz} \right) \\
&= -\text{Tr} \left(\Phi^{-1} \frac{d \Phi}{dz} \right) - \text{Tr} \left(\mathcal{G}_{\mathbf{D}} \frac{d \tilde{\Phi}}{dz} \right). \tag{79}
\end{aligned}$$

Similarly, we can get the following equations

$$\begin{aligned}
& \text{Tr} \left(\left(\Delta - \tilde{\Phi}^{-1} \right)^{-1} \frac{d(-\Delta)}{dz} \right) \\
&= \text{Tr} \left(\left(\Delta - \tilde{\Phi}^{-1} \right)^{-1} \frac{d \left(\bar{\mathbf{G}}^\dagger \tilde{\Psi} \bar{\mathbf{G}} - \Psi \right)}{dz} \right) \\
&= \text{Tr} \left(\mathcal{G}_{\mathbf{C}} \frac{d \left(\bar{\mathbf{G}}^\dagger \tilde{\Psi} \bar{\mathbf{G}} \right)}{dz} \right) - \text{Tr} \left(\mathcal{G}_{\mathbf{C}} \frac{d \Psi}{dz} \right) - \text{Tr} \left(\mathcal{G}_{\mathbf{D}} \frac{d \tilde{\Phi}}{dz} \right) + \text{Tr} \left(\left(\tilde{\Phi} - \Delta^{-1} \right)^{-1} \frac{d \tilde{\Phi}}{dz} \right), \tag{80}
\end{aligned}$$

$$\begin{aligned}
& \text{Tr} \left(\left(\tilde{\Phi} - \Delta^{-1} \right)^{-1} \frac{d \tilde{\Phi}}{dz} \right) \\
&= \text{Tr} \left(\tilde{\Phi}^{-1} \frac{d \tilde{\Phi}}{dz} \right) - \text{Tr} \left(\left(\Delta - \tilde{\Phi}^{-1} \right)^{-1} \frac{d \tilde{\Phi}^{-1}}{dz} \right). \tag{81}
\end{aligned}$$

Then (73) can be expressed as

$$\begin{aligned}
& \frac{d}{dz} \log \det \left(-\tilde{\Phi}^{-1} + \Delta \right) \\
&= -\text{Tr} \left(\left(\Delta - \tilde{\Phi}^{-1} \right)^{-1} \frac{d(-\Delta)}{dz} \right) - \text{Tr} \left(\left(\Delta - \tilde{\Phi}^{-1} \right)^{-1} \frac{d\tilde{\Phi}^{-1}}{dz} \right), \\
&= -\text{Tr} \left(\mathcal{G}_{\mathbf{C}} \frac{\left(\overline{\mathbf{G}}^\dagger \tilde{\Psi} \overline{\mathbf{G}} \right)}{dz} \right) + \text{Tr} \left(\mathcal{G}_{\mathbf{C}} \frac{d\Psi}{dz} \right) + \text{Tr} \left(\mathcal{G}_{\mathbf{D}} \frac{d\tilde{\Phi}}{dz} \right) - \text{Tr} \left(\tilde{\Phi}^{-1} \frac{d\tilde{\Phi}}{dz} \right). \tag{82}
\end{aligned}$$

Combining (72), (74), (75), (78), (79), (82), we have

$$\frac{d}{dz} \mathcal{V}_{\mathbf{B}_1}(z) = -\frac{1}{z} - \frac{1}{LN_r} \text{Tr}(\mathcal{G}_{\tilde{\mathbf{C}}}) = -\frac{1}{z} - \mathcal{G}_{\mathbf{B}_1}(-z), \tag{83}$$

and the proof of Proposition 2 is completed.

REFERENCES

- [1] J. A. Zhang, M. L. Rahman, K. Wu, X. Huang, Y. J. Guo, S. Chen, and J. Yuan, "Enabling joint communication and radar sensing in mobile networks—a survey," *IEEE Commun. Surveys Tuts.*, vol. 24, no. 1, pp. 306–345, 2021.
- [2] F. Liu, C. Masouros, A. Li, H. Sun, and L. Hanzo, "Mu-MIMO communications with MIMO radar: From co-existence to joint transmission," *IEEE Trans. Wireless Commun.*, vol. 17, no. 4, pp. 2755–2770, 2018.
- [3] X. Wang, Z. Fei, J. A. Zhang, and J. Xu, "Partially-connected hybrid beamforming design for integrated sensing and communication systems," *IEEE Trans. Commun.*, vol. 70, no. 10, pp. 6648–6660, 2022.
- [4] M. Al-Jarrah, E. Alsusa and C. Masouros, "A Unified Performance Framework for Integrated Sensing-Communications Based on KL-Divergence," *IEEE Trans. Wireless Commun.*, vol. 22, no. 12, pp. 9390-9411, Dec. 2023.
- [5] Z. Fei, S. Tang, X. Wang, F. Xia, F. Liu and J. Andrew Zhang, "Revealing the Trade-Off in ISAC Systems: The KL Divergence Perspective," *IEEE Wireless Commun. Lett.*, vol. 13, no. 10, pp. 2747-2751, Oct. 2024.
- [6] R. Xu, L. Peng, W. Zhao, and Z. Mi, "Radar mutual information and communication channel capacity of integrated radar-communication system using MIMO," *ICT Express*, vol. 1, no. 3, pp. 102–105, 2015.
- [7] Y. Liu, G. Liao, and Z. Yang, "Robust OFDM integrated radar and communications waveform design based on information theory," *Signal Process.*, vol. 162, pp. 317–329, 2019.
- [8] M. Dai and B. Clerckx, "Multiuser millimeter wave beamforming strategies with quantized and statistical CSIT," *IEEE Trans. Wireless Commun.*, vol. 16, no. 11, pp. 7025–7038, 2017.
- [9] J. Dang, Z. Zhang, and L. Wu, "Joint beamforming for intelligent reflecting surface aided wireless communication using statistical CSI," *China Commun.*, vol. 17, no. 8, pp. 147–157, 2020.
- [10] W. Weichselberger, M. Herdin, H. Ozelik, and E. Bonek, "A stochastic MIMO channel model with joint correlation of both link ends," *IEEE Trans. Wireless Commun.*, vol. 5, no. 1, pp. 90–100, 2006.
- [11] Y. Xu, Y. Li, J. A. Zhang, M. Di Renzo, and T. Q. Quek, "Joint beamforming for RIS-assisted integrated sensing and communication systems," *IEEE Trans. Commun.*, 2023.
- [12] Hoydis, Jakob, Romain Couillet, and Mérouane Debbah. "Asymptotic analysis of double-scattering channels." 2011 Conference Record of the Forty Fifth Asilomar Conference on Signals, Systems and Computers (ASILOMAR). IEEE, 2011.
- [13] A. M. Tulino and S. Verdú, "Random matrix theory and wireless communications," *Found. Trends Commun. Inf. Theory*, vol. 1, pp. 1–182, Jun. 2004, Now Publishers.
- [14] R. R. Müller, "On the asymptotic eigenvalue distribution of concatenated vector-valued fading channels," *IEEE Trans. Inf. Theory*, vol. 48, no. 7, pp. 2086–2091, 2002.
- [15] S. T. Belinschi, T. Mai, and R. Speicher, "Analytic subordination theory of operator-valued free additive convolution and the solution of a general random matrix problem," *J. Reine Angew. Math. (Crelles J.)*, vol. 2017, no. 732, pp. 21–53, 2017.
- [16] Silverstein, J. W., "Strong convergence of the empirical distribution of eigenvalues of large dimensional random matrices," *Journal of Multivariate Analysis*, vol. 55, no. 2, pp. 331-339, 1995.

- [17] Z. Zheng, S. Wang, Z. Fei, Z. Sun, and J. Yuan, "On the mutual information of multi-RIS assisted MIMO: From operator-valued free probability aspect," *IEEE Trans. Commun.*, vol. 71, no. 12, pp. 6952-6966, 2023.
- [18] S. Wang, Z. Zheng, Z. Fei, J. Guo, J. Yuan and Z. Sun, "Toward Ergodic Sum Rate Maximization of Multiple-RIS-Assisted MIMO Multiple Access Channels Over Generic Rician Fading," *IEEE Trans. Wireless Commun.*, vol. 23, no. 8, pp. 9613-9628, 2024